研究成果刊行に関する一覧表

＊雑誌

発表者氏名	論文タイトル	発表誌名	巻号	ページ	出版年（西暦）
Ishiura H, Sako W, Yoshida M, Nakagawa M, Kaji R, Tsuji S, et al.	The TRK-fused gene is mutated in hereditary motor and sensory neuropathy with proximal dominant involvement.	Am J Hum Genet	91	320-329	2012
中川正法	Charcot-Marie-Tooth 病 1.病態・治療。	最新医学　別冊 新しい診断と治療の ABC75　末梢神経障害		152-160	2012
中川正法	Charcot-Marie-Tooth 病に対する治療の進歩	Annual　review 神経		211-222	2013
渡邉耕太，木井雄一郎，鈴木智之，寺本篤史，山下敏彦	骨・関節のバイオメカニクス―最近の進歩．足・足関節のバイオメカニクス―足部アライメントの荷重による変化の検討―	整・災外	55	1417-1421	2012
木井雄一郎，鈴木智之，渡邉耕太，寺本篤史，山下敏彦	足部縦アーチの荷重による変化の検討：CT による3次元解析	靴の医学	25	155-159	2012
寺本篤史，吉本正太，木井雄一郎，渡邉耕太，山下敏彦，杉 憲	足関節底背屈がCTにおける距腿関節窩と脛腓靱帯結合に及ぼす影響	日足外会誌	33	101-105	2012
Watanabe K, Fujii T, Kitaoka HB, Kotajarvi BR, Luo ZP, An KN.	Analysis of Ankle-Hindfoot Stability in Patients with Ankle Instability and Normals.	Int Orthop	36	89-94	2012
Watanabe K, Kitaoka HB, Berglund LJ, Zhao KD, Kaufman KR, An KN.	The role of ankle ligaments and articular geometry in stabilizing the ankle.	Clin Biomech	27	189-195	2012

研究成果刊行に関する一覧表

発表者氏名	論文タイトル	発表誌名	巻号	ページ	出版年 （西暦）
蜂須賀明子，松嶋康之，蜂須賀研二	腕神経叢損傷後の複合性局所疼痛症候群にドラッグチャレンジテストが有用であった1例	The Japanese Journal of Rehabilitation Medicine	49	512-517	2012
伊藤英明, 松嶋康之, 佐伯覚，蜂須賀研二	ポストポリオ症候群のリハビリテーション	総合リハ	40	675-679	2012
Kensuke Shiga, Yuichi Noto, Ikuko Mizuta, Akihiro Hashiguchi, Hiroshi Takashima, Masanori Nakagawa	A Novel EGR2 mutation within a family with a mild demyelinating form of Charcot-Marie-Tooth disease	J Periph Nerv Syst	17	206-209	2012
Kensuke Shiga, Yukiko Tsuji, Chihiro Fujii, Yu-ichi Noto, Masanori Nakagawa	Demyelinating features in sensory nerve conduction in Fisher syndrome	Intern Med	51	2307-2312	2012
Kensuke Shiga, Eijiroh Tanaka, Reina Isayama, Toshiki Mizuno, Kyoko Itoh, Masanori Nakagawa	Chronic inflammatory demyelinating polyneuropathy due to the administration of pegylated interferon-α2b：a neuropathology case report.	Intern Med	51	217-221	2012

研究成果刊行に関する一覧表

＊書籍

著者氏名	論　文タイトル名	書籍全体の編集者名	書籍名	出版社名	出版地	出版年	ページ
蜂須賀研二，和田太	腎不全に伴う末梢神経障害例へのリハビリテーション	上月正博	腎臓リハビリテーション. 第1版	医歯薬出版	東京	2012	414-419
蜂須賀研二	ポリオ後症候群	伊藤利之，大橋正洋，千田富義，永田雅章	標準リハビリテーション医学. 第3版	医学書院	東京	2012	387-388

REPORT

The TRK-Fused Gene Is Mutated in Hereditary Motor and Sensory Neuropathy with Proximal Dominant Involvement

Hiroyuki Ishiura,[1] Wataru Sako,[3] Mari Yoshida,[4] Toshitaka Kawarai,[3] Osamu Tanabe,[3,5] Jun Goto,[1] Yuji Takahashi,[1] Hidetoshi Date,[1] Jun Mitsui,[1] Budrul Ahsan,[1] Yaeko Ichikawa,[1] Atsushi Iwata,[1] Hiide Yoshino,[6] Yuishin Izumi,[3] Koji Fujita,[3] Kouji Maeda,[3] Satoshi Goto,[3] Hidetaka Koizumi,[3] Ryoma Morigaki,[3] Masako Ikemura,[7] Naoko Yamauchi,[7] Shigeo Murayama,[8] Garth A. Nicholson,[9] Hidefumi Ito,[10] Gen Sobue,[11] Masanori Nakagawa,[12] Ryuji Kaji,[3,*] and Shoji Tsuji[1,2,13,*]

Hereditary motor and sensory neuropathy with proximal dominant involvement (HMSN-P) is an autosomal-dominant neurodegenerative disorder characterized by widespread fasciculations, proximal-predominant muscle weakness, and atrophy followed by distal sensory involvement. To date, large families affected by HMSN-P have been reported from two different regions in Japan. Linkage and haplotype analyses of two previously reported families and two new families with the use of high-density SNP arrays further defined the minimum candidate region of 3.3 Mb in chromosomal region 3q12. Exome sequencing showed an identical c.854C>T (p.Pro285-Leu) mutation in the TRK-fused gene (TFG) in the four families. Detailed haplotype analysis suggested two independent origins of the mutation. Pathological studies of an autopsied patient revealed TFG- and ubiquitin-immunopositive cytoplasmic inclusions in the spinal and cortical motor neurons. Fragmentation of the Golgi apparatus, a frequent finding in amyotrophic lateral sclerosis, was also observed in the motor neurons with inclusion bodies. Moreover, TAR DNA-binding protein 43 kDa (TDP-43)-positive cytoplasmic inclusions were also demonstrated. In cultured cells expressing mutant TFG, cytoplasmic aggregation of TDP-43 was demonstrated. These findings indicate that formation of TFG-containing cytoplasmic inclusions and concomitant mislocalization of TDP-43 underlie motor neuron degeneration in HMSN-P. Pathological overlap of proteinopathies involving TFG and TDP-43 highlights a new pathway leading to motor neuron degeneration.

Hereditary motor and sensory neuropathy with proximal dominant involvement (HMSN-P [MIM 604484]) is an autosomal-dominant disease characterized by predominantly proximal muscle weakness and atrophy followed by distal sensory disturbances.[1] HMSN-P was first described in patients from the Okinawa Islands of Japan, where more than 100 people are estimated to be affected.[2] Two Brazilian HMSN-P-affected families of Okinawan ancestry have also been reported.[3,4]

The disease onset is usually in the 40s and is followed by a slowly progressive course. Painful muscle cramps and abundant fasciculations are observed, particularly in the early stage of the disease. In contrast to the clinical presentations of other hereditary motor and sensory neuropathies (HMSNs) presenting with predominantly distal motor weakness reflecting axonal-length dependence, the clinical presentation of HMSN-P is unique in that it involves proximal predominant weakness with widespread fasciculations resembling those of amyotrophic lateral sclerosis (ALS).[5] Distal sensory loss is accompanied later
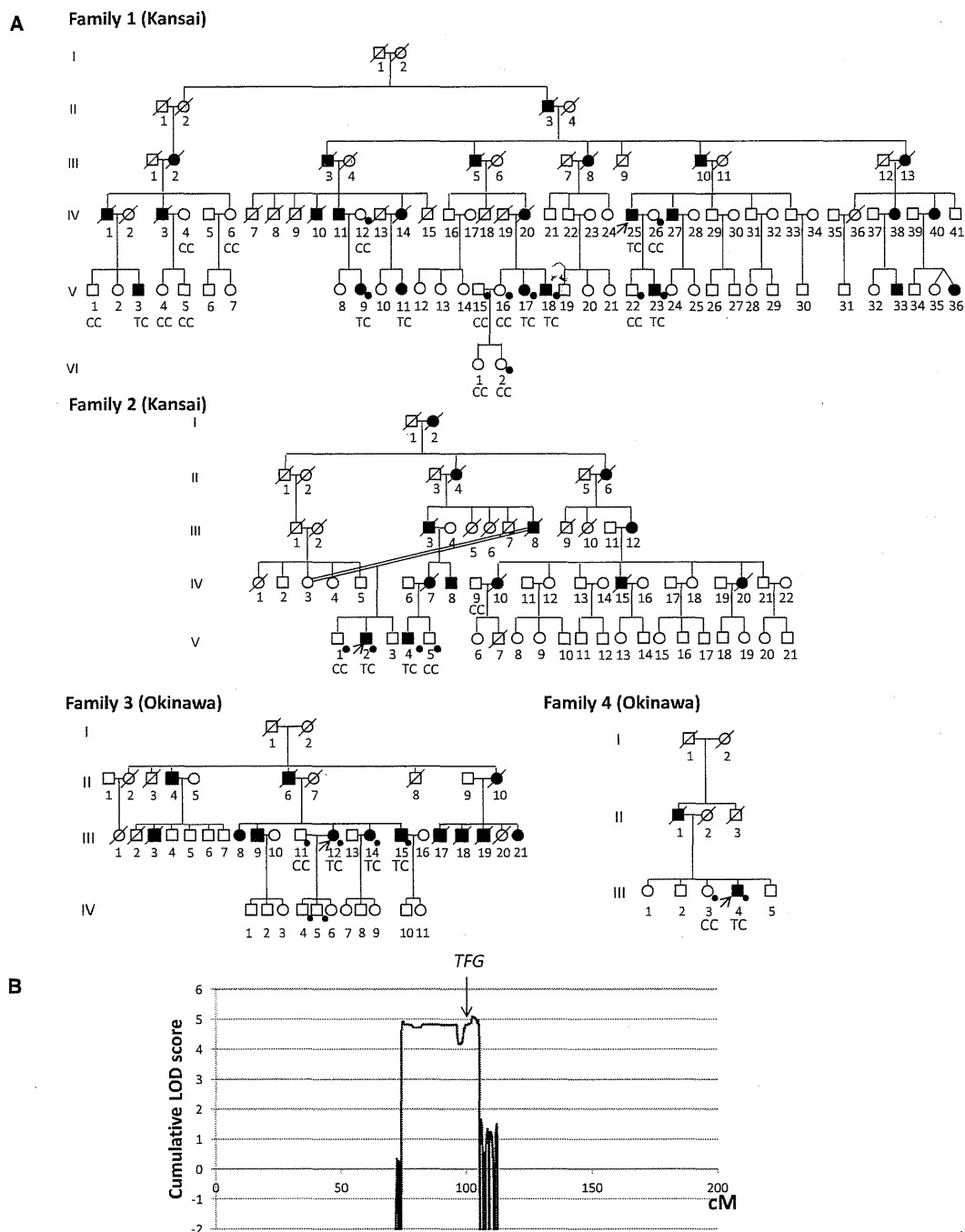
in the disease course, but the degree of the sensory involvement varies among patients. Neuropathological findings revealed severe neuronal loss and gliosis in the spinal anterior horns and mild neuronal loss and gliosis in the hypoglossal and facial nuclei of the brainstem, which indicates that the primary pathological feature of HMSN-P is a motor neuronopathy involving motor neurons, but not a motor neuropathy involving axons.[1,5] The posterior column, corticospinal tract, and spinocerebellar tract showed loss of myelinated fibers and gliosis. Neuronal loss and gliosis were found in Clarke's nucleus. Dorsal root ganglia showed mild to marked neuronal loss.[1,5] These observations suggest that HMSN-P shares neuropathological findings in part with those observed in familial ALS.[6]

Previous studies on Okinawan kindreds mapped the disease locus to chromosome 3q.[1] Subsequently, we identified two large families (families 1 and 2 in Figure 1A) affected by quite a similar phenotype in the Kansai area of Japan, located in the middle of the main island of Japan and far distant from the Okinawa Islands. We mapped the

Figure 1. Pedigree Charts and Linkage Analysis
(A) Pedigree charts of families 1 and 2 (Kansai kindreds) and families 3 and 4 (Okinawan kindreds) are shown. Squares and circles indicate males and females, respectively. Affected persons are designated with filled symbols. A diagonal line through a symbol represents a deceased person. A person with an arrow is an index patient. Genotypes of *TFG* c.854 are shown in individuals in whom genomic DNA was analyzed. Individuals genotyped with SNP arrays for linkage analysis and haplotype reconstruction are indicated by dots.
(B) Cumulative parametric multipoint LOD scores on chromosome 3 of all the families are shown.

disease locus to chromosome 3q,[7] overlapping with the previously defined locus, which strongly indicates that these diseases are indeed identical.

In addition to the large Kansai HMSN-P-affected families, we found two new Okinawan HMSN-P-affected families (families 3 and 4 in Figure 1A) in our study. In total, 9 affected and 15 unaffected individuals from the Kansai area and four affected and four unaffected individuals from the Okinawa Islands were enrolled in the study. Written informed consent was obtained from

Table 1. Clinical Characteristics of Patients with HMSN-P from Families 1 and 2 from Kansai and Families 3 and 4 from Okinawa

| | Families 1 and 2 | Family 3 | | | Family 4 |
		III-12	III-14	III-15	III-4
Age at examination (years)	40s–50s	54	52	50	54
Age at onset (years)	37.5 ± 8	44	40	early 20s	41
Initial symptoms	shoulder dislocation and difficulty walking	proximal leg weakness	painful cramps	painful cramps and fasciculation	painful cramps and calf atrophy
Motor					
Proximal muscle weakness and atrophy	+	+	mild	+	+
Painful cramps	+	+	+	+	+
Fasciculations	+	+	+	+	+
Motor ability	bedridden after 10–20 years from disease onset	unable to walk; wheelchair	only mild difficulty climbing stairs	walk with effort	unable to walk; wheelchair
Bulbar symptoms	– ~ +	–	–	–	–
Sensory					
Dysesthesia	+	+	mild	+	+
Decreased tactile sensation	+	+	–	mild	+
Decreased vibratory sensation	+	mild	mild	mild	+
Reflexes					
Tendon reflexes	diminished	diminished	diminished	diminished	diminished
Pathological reflexes	–	–	–	–	–
Laboratory Tests and Electrophysiological Findings					
Serum creatine kinase level	270 ± 101 IU/l	761 IU/l	not measured	625 IU/l	399 IU/l
Hyperglycemia	4/13 patients	–	–	–	+
Hyperlipidemia	3/13 patients	+	–	+	+
Nerve conduction study	motor and sensory axonal degeneration	motor and sensory axonal degeneration	not examined	not examined	motor and sensory axonal degeneration
Needle electromyography	neurogenic changes with fibrillation potentials and positive sharp waves	neurogenic changes with fibrillation potentials and positive sharp waves	not examined	not examined	not examined

The clinical characteristics of the patients from families 1 and 2 were summarized in accordance with the previous studies.[5,6]

all participants. This study was approved by the institutional review boards at the University of Tokyo and the Tokushima University Hospital. Genomic DNA was extracted from peripheral-blood leukocytes or an autopsied brain according to standard procedures.

The clinical presentations of the patients from the four families are summarized in Table 1 and Table S1, available online. Characteristic painful cramps and fasciculations were noted at the initial stage of the disease in all the patients from the four families. Whereas some of the patients showed painful cramps in their 20s, the ages of onset of motor weakness (41.6 ± 2.9 years old) were quite uniform. These patients presented slowly progressive, predominantly proximal weakness and atrophy with dimin-

ished tendon reflexes in the lower extremities. Sensory impairment was generally mild. Indeed, one patient (III-4 in family 4) has been diagnosed with very slowly progressive ALS. Although frontotemporal dementia (FTD) is an occasionally observed clinical presentation in patients with ALS, dementia was not observed in these patients. Laboratory tests showed mildly elevated serum creatine kinase levels. Electrophysiological studies showed similar results in all the patients investigated and revealed a decreased number of motor units with abundant positive sharp waves, fibrillation, and fasciculation potentials. Sensory-nerve action potentials of the sural nerve were lost in the later stage of the disease. All these clinical findings were similar to those described in previous reports.[1,3,4]

To further narrow the candidate region, we conducted detailed genotyping by employing the Genome-Wide Human SNP array 6.0 (Affymetrix). Multipoint parametric linkage analysis and haplotype reconstruction were performed with the pipeline software SNP-HiTLink[8] and Allegro v.2[9] (Figure 1A). In addition to the SNP genotyping, we also used newly discovered polymorphic dinucleotide repeats for haplotype comparison (microsatellite marker 1 [MS1], chr3: 101,901,207–101,901,249; and MS2, chr3: 102,157,749–102,157,795 in hg18) around *TFG* (see Table S2 for primer sequences). The genome-wide linkage study revealed only one chromosome 3 region showing a cumulative LOD score exceeding 3.0 (Figure 1B), confirming the result of our previous study.[7] An obligate recombination event was observed between rs4894942 and rs1104964, thus further refining the telomeric boundary of the candidate region in Kansai families (Figure 2A). The Okinawan families (families 3 and 4) shared an extended disease haplotype spanning 3.3 Mb, consistent with a founder effect reported in the Okinawan HMSN-P-affected families,[1] thus defining the 3.3 Mb region as the minimum candidate region.

We then performed exon capture (Sequence Capture Human Exome 2.1 M Array [NimbleGen]) of the index patient from family 3 and subsequent passively parallel sequencing by using two lanes of GAIIx (100 bp single end [Illumina]) and a one-fifth slide of SOLiD 4 (50 bp single end [Life Technologies]). GAIIx and SOLiD4 yielded 2.60 and 2.76 Gb of uniquely mapped reads,[10] respectively. The average coverages were 29.0× and 26.8× in GAIIx and SOLiD4, respectively (Table S3 and Figure S1). In summary, 175,236 single nucleotide variants (SNVs) and 25,987 small insertions/deletions were called.[11] The numbers of exonic and splice-site variants were 14,189 and 127, respectively. In the minimum candidate region of 3.3 Mb, only 11 exonic SNVs were found, and only one was novel (i.e., not found in dbSNP) and nonsynonymous. Direct nucleotide-sequence analysis confirmed the presence of heterozygous SNV c.854C>T (p.Pro285Leu) in TRK-fused gene (*TFG* [NM_006070.5]) in all the patients from families 3 and 4 (Figure 3A and Figure S2[12]). Intriguingly, direct nucleotide-sequence analysis of all *TFG* exons (see Table S4 for primer sequences) of one patient from each of families 1 and 2 from the Kansai area revealed an identical c.854C>T (p.Pro285Leu) *TFG* mutation cosegregating with the disease (Figure 1A and Figure 3A). The base substitution was not observed in 482 Japanese controls (964 chromosomes), dbSNP, the 1000 Genomes Project Database, or the Exome Sequencing Project Database. Pro285 is located in the P/Q-rich domain in the C-terminal region of TFG (Figure 3B) and is evolutionarily conserved (Figure 3C). PolyPhen predicts it to be "probably damaging." Because some of the exonic sequences were not sufficiently covered by exome sequencing (i.e., their read depths were no more than 10×) (Figure S1), direct nucleotide-sequence analysis was further conducted for these exonic sequences (Table S5). However, it did not reveal any other novel

nonsynonymous variants, confirming that c.854C>T (p.Pro285Leu) is the only mutation exclusively present in the candidate region of 3.3 Mb. All together, we concluded that it was the disease-causing mutation.
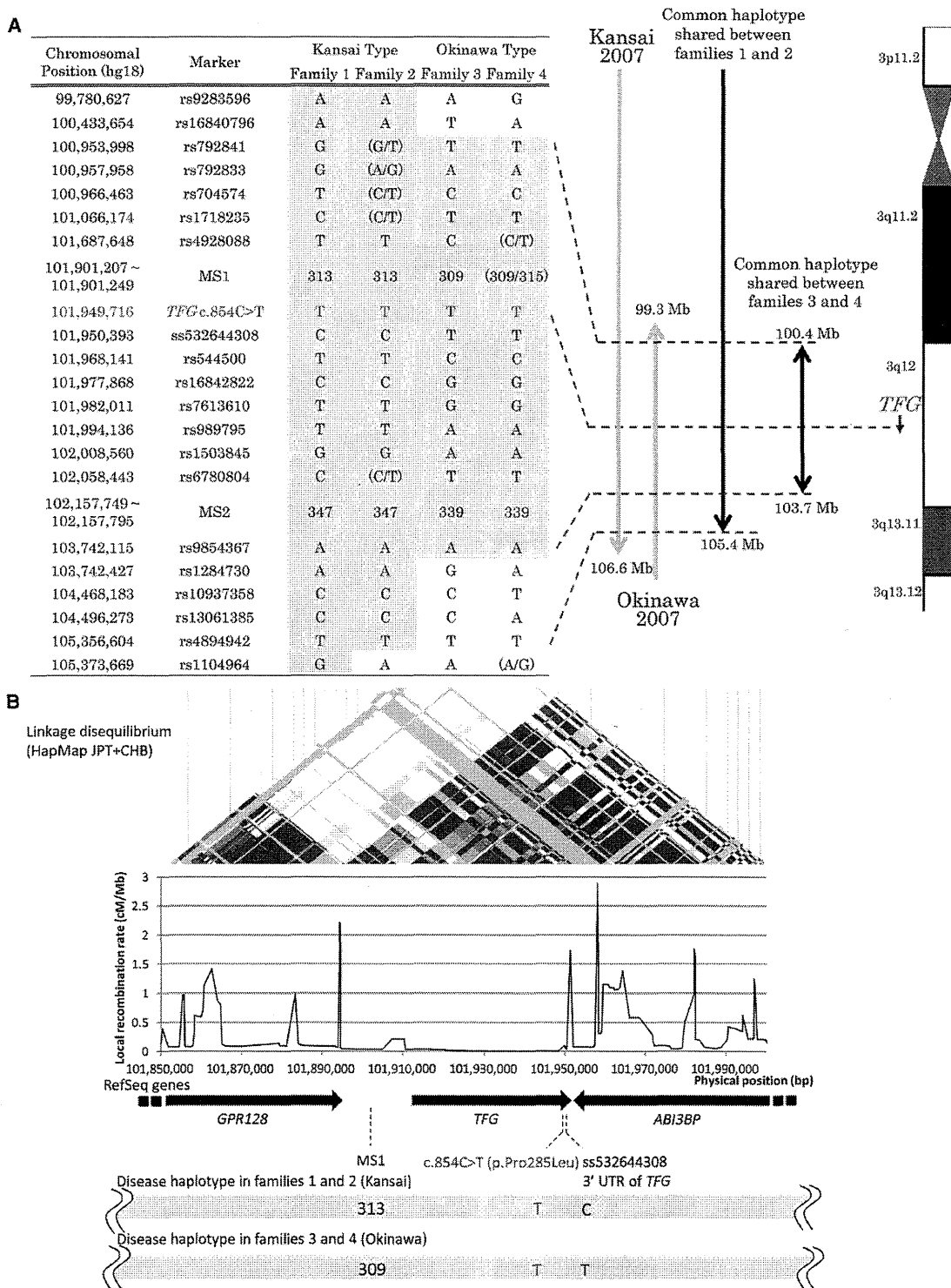
Because we found an identical mutation in both Kansai (families 1 and 2) and Okinawan (families 3 and 4) families, we then compared the haplotypes with the c.854C>T (p.Pro285Leu) mutation in the Kansai and Okinawan families in detail. To obtain high-resolution haplotypes, we included custom-made markers, including MS1 and MS2, and new SNVs identified by our exome analysis, in addition to the high-density SNPs used in the linkage analysis. The two Kansai families shared as long as 24.0 Mb of haplotype, and the two Okinawan families shared 3.3 Mb, strongly supporting a common ancestry in each region. When the haplotypes of the Kansai and Okinawan families were compared, it turned out that these families do not share the same haplotype because the markers nearest to *TFG* are discordant at markers 48.5 kb centromeric and 677 bp telomeric to the mutation within a haploblock (Figure 2B). Although the possibility of rare recombination events just distal to the mutation cannot be completely excluded, as suggested by the population-based recombination map (Figure 2B), these findings strongly support the interpretation that the mutations have independent origins and provide further evidence that *TFG* contains the causative mutation for this disease.

Mutational analyses of *TFG* were further conducted in patients with other diseases affecting lower motor neurons (including familial ALS [n = 18], axonal HMSN [n = 26], and hereditary motor neuropathy [n = 3]) and revealed no mutations in *TFG*, indicating that c.854C>T (p.Pro285-Leu) in *TFG* is highly specific to HMSN-P.

In this study, we identified in all four families a single variant that appears to have developed on two different haplotypes. The mutation disrupts the PXXP motif, also known as the Src homology 3 (SH3) domain, which might affect protein-protein interactions. In addition, substitution of leucine for proline is expected to markedly alter the protein's secondary structure, which might substantially compromise the physiological functions of TFG.

By employing the primers shown in Table S6, we obtained full-length cDNAs by PCR amplification of the cDNAs prepared from a cDNA library of the human fetal brain (Clontech). During this process, four species of cDNA were identified (Figure S3A). To determine the relative abundance of these cDNA species, we used the primers shown in Table S7 to conduct fragment analysis of the RT-PCR products obtained from RNAs extracted from various tissues; these primers were designed to discriminate four cDNA species on the basis of the size of the PCR products. The analysis revealed that TFG is ubiquitously expressed, including in the spinal cord and dorsal root ganglia, which are the affected sites of HMSN-P (Figure S3B).
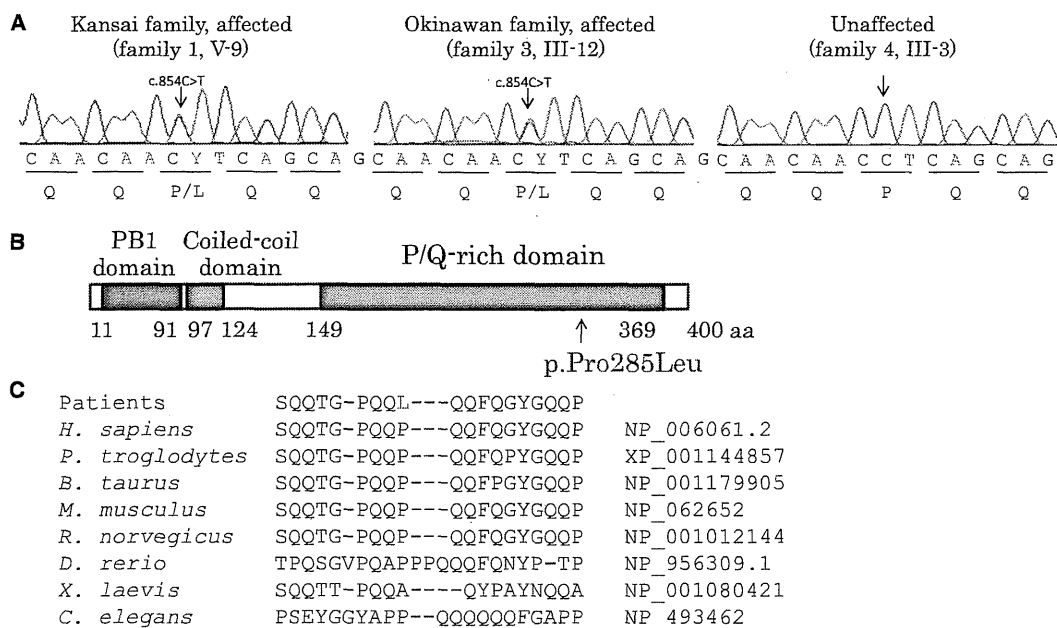
Neuropathological studies were performed in a *TFG*-mutation-positive patient (IV-25 in family 1) who died of

A

Chromosomal Position (hg18)	Marker	Kansai Type Family 1	Kansai Type Family 2	Okinawa Type Family 3	Okinawa Type Family 4
99,780,627	rs9283596	A	A	A	G
100,433,654	rs16840796	A	A	T	A
100,953,998	rs792841	G	(G/T)	T	T
100,957,958	rs792833	G	(A/G)	A	A
100,966,463	rs704574	T	(C/T)	C	C
101,066,174	rs1718235	C	(C/T)	T	T
101,687,648	rs4928088	T	T	C	(C/T)
101,901,207 ~ 101,901,249	MS1	313	313	309	(309/315)
101,949,716	TFG c.854C>T	T	T	T	T
101,950,393	ss532644308	C	C	T	T
101,968,141	rs544500	T	T	C	C
101,977,868	rs16842822	C	C	G	G
101,982,011	rs7613610	T	T	G	G
101,994,136	rs989795	T	T	A	A
102,008,560	rs1503845	G	G	A	A
102,058,443	rs6780804	C	(C/T)	T	T
102,157,749 ~ 102,157,795	MS2	347	347	339	339
103,742,115	rs9854367	A	A	A	A
103,742,427	rs1284730	A	A	G	A
104,468,183	rs10937358	C	C	C	T
104,496,273	rs13061385	C	C	C	A
105,356,604	rs4894942	T	T	T	T
105,373,669	rs1104964	G	A	A	(A/G)

Common haplotype shared between families 1 and 2 — Kansai 2007

99.3 Mb

Common haplotype shared between familes 3 and 4

100.4 Mb

103.7 Mb

105.4 Mb

106.6 Mb — Okinawa 2007

3p11.2

3q11.2

3q12

TFG

3q13.11

3q13.12

B

Linkage disequilibrium (HapMap JPT+CHB)

Local recombination rate (cM/Mb)

101,850,000   101,870,000   101,890,000   101,910,000   101,930,000   101,950,000   101,970,000   101,990,000

Physical position (bp)

RefSeq genes

GPR128   TFG   ABI3BP

MS1   c.854C>T (p.Pro285Leu) ss532644308
3′ UTR of TFG

Disease haplotype in families 1 and 2 (Kansai)

313   T   C

Disease haplotype in families 3 and 4 (Okinawa)

309   T   T

Figure 2.   Haplotype Analysis and Minimum Candidate Region of HMSN-P
(A) Haplotypes were reconstructed for all the families with the use of SNP array data and microsatellite markers. Previously reported candidate regions are shown as "Kansai 2007" and "Okinawa 2007."[1,6] Because families 1 and 2 are distantly related, an extended shared common haplotype was observed on chromosome 3, as indicated by a previous study.[6] A reassessment of linkage analysis with high-density SNP markers revealed a recombination between rs4894942 and rs1104964 in family 2, thus refining the telomeric boundary of the candidate region in Kansai families (designated as "Common haplotype shared between families 1 and 2). Furthermore, a shared common haplotype (3.3 Mb with boundaries at rs16840796 and rs1284730) between families 3 and 4 was found, defining the minimum candidate region.

A Kansai family, affected   Okinawan family, affected   Unaffected
   (family 1, V-9)   (family 3, III-12)   (family 4, III-3)

c.854C>T   c.854C>T   ↓

C A A C A A C Y T C A G C A   G C A A C A A C Y T C A G C A   G C A A C A A C C T C A G C A G

Q   Q   P/L   Q   Q   G   Q   Q   P/L   Q   Q   Q   Q   P   Q   Q

B   PB1   Coiled-coil
      domain   domain   P/Q-rich domain

      11   91 97 124   149   ↑   369   400 aa
                                           p.Pro285Leu

C
Patients		
	SQQTG-PQQL---QQFQGYGQQP	
H. sapiens	SQQTG-PQQP---QQFQGYGQQP	NP_006061.2
P. troglodytes	SQQTG-PQQP---QQFQPYGQQP	XP_001144857
B. taurus	SQQTG-PQQP---QQFPGYGQQP	NP_001179905
M. musculus	SQQTG-PQQP---QQFQGYGQQP	NP_062652
R. norvegicus	SQQTG-PQQP---QQFQGYGQQP	NP_001012144
D. rerio	TPQSGVPQAPPPQQQFQNYP-TP	NP_956309.1
X. laevis	SQQTT-PQQA----QYPAYNQQA	NP_001080421
C. elegans	PSEYGGYAPP--QQQQQQFGAPP	NP_493462

Figure 3. Identification of Causative Mutation
(A) Exome sequencing revealed that only one novel nonsynonymous variant is located within the minimum candidate region. Direct nucleotide-sequence analysis confirmed the mutation, c.854C>T (p.Pro285Leu), in TFG in both Kansai and Okinawan families. The mutation cosegregated with the disease (Figure 1A).
(B) Schematic representation of TFG isoform 1. The alteration (p.Pro285Leu) detected in this study is shown below.
(C) Cross-species homology search of the partial TFG amino acid sequence containing the p.Pro285Leu alteration revealed that Pro285 is evolutionarily conserved among species.

pneumonia at 67 years of age.[5] Immunohistochemical observations employing a TFG antibody (Table S8) revealed fine granular immunostaining of TFG in the cytoplasm of motor neurons in the spinal cord of neurologically normal controls (n = 3; age at death = 58.7 ± 19.6 years old) (Figure 4A). In the HMSN-P patient, in contrast, TFG-immunopositive inclusion bodies were detected in the motor neurons of the facial, hypoglossal, and abducens nuclei and the spinal cord, as well as in the sensory neurons of the dorsal root ganglia, but were not detected in glial cells (Figures 4B–4D). A small number of cortical neurons in the precentral gyrus also showed TFG-immunopositive inclusion bodies (Figure 4E). Serial sections stained with antibodies against ubiquitin or TFG (Figure 4F) and double immunofluorescence staining (Figure 4G) demonstrated that TFG-immunopositive inclusions colocalized with ubiquitin deposition. Inclusion bodies were immunopositive for optineurin in motor neurons of the brainstem nuclei and the anterior horn of the spinal cord,[5] as well as in sensory neurons of the dorsal root ganglia (data not shown). These data strongly indicate that HMSN-P is a proteinopathy involving TFG.

Because HMSN-P and ALS share some clinical characteristics, we then examined whether neuropathological findings of HMSN-P shared cardinal features with those of sporadic ALS.[13–16] Immunohistochemistry with a TDP-43 antibody revealed skein-like inclusions in the remaining motor neurons of the abducens nucleus and the anterior horn of the lumbar cord (Figures 4H–4I). Phosphorylated TDP-43-positive inclusions were also identified in neurons of the anterior horn of the cervical cord and Clarke's nucleus (Figures 4J–4K). In contrast, TFG immunostaining of spinal-cord specimens from four patients with sporadic ALS (their age at death was 72.3 ± 7.4 years old) revealed no pathological staining in the motor neurons (data not shown). Double immunofluorescence staining revealed that many of the TFG-immunopositive round inclusions in the HSMN-P patient were negative for TDP-43 (Figure 4L), whereas a small number of inclusions were positive for both TFG and TDP-43 (Figure 4M). In addition, to investigate morphological Golgi-apparatus changes, which have recently been found in motor neurons of autopsied tissues of ALS patients,[17] we conducted immunohistochemical analysis by using

(B) Disease haplotypes in the Kansai and Okinawan kindreds are indicated below. Local recombination rates, RefSeq genes, and the linkage disequilibrium map from HapMap JPT (Japanese in Tokyo, Japan) and CHB (Han Chinese in Beijing, China) samples are shown above the disease haplotypes. When disease haplotypes of the Kansai and Okinawan kindreds are compared, the markers nearest to TFG are discordant at markers 48.5 kb centromeric and 677 bp telomeric to the mutation within a haploblock, strongly supporting the interpretation that the mutations have independent origins.

-29-
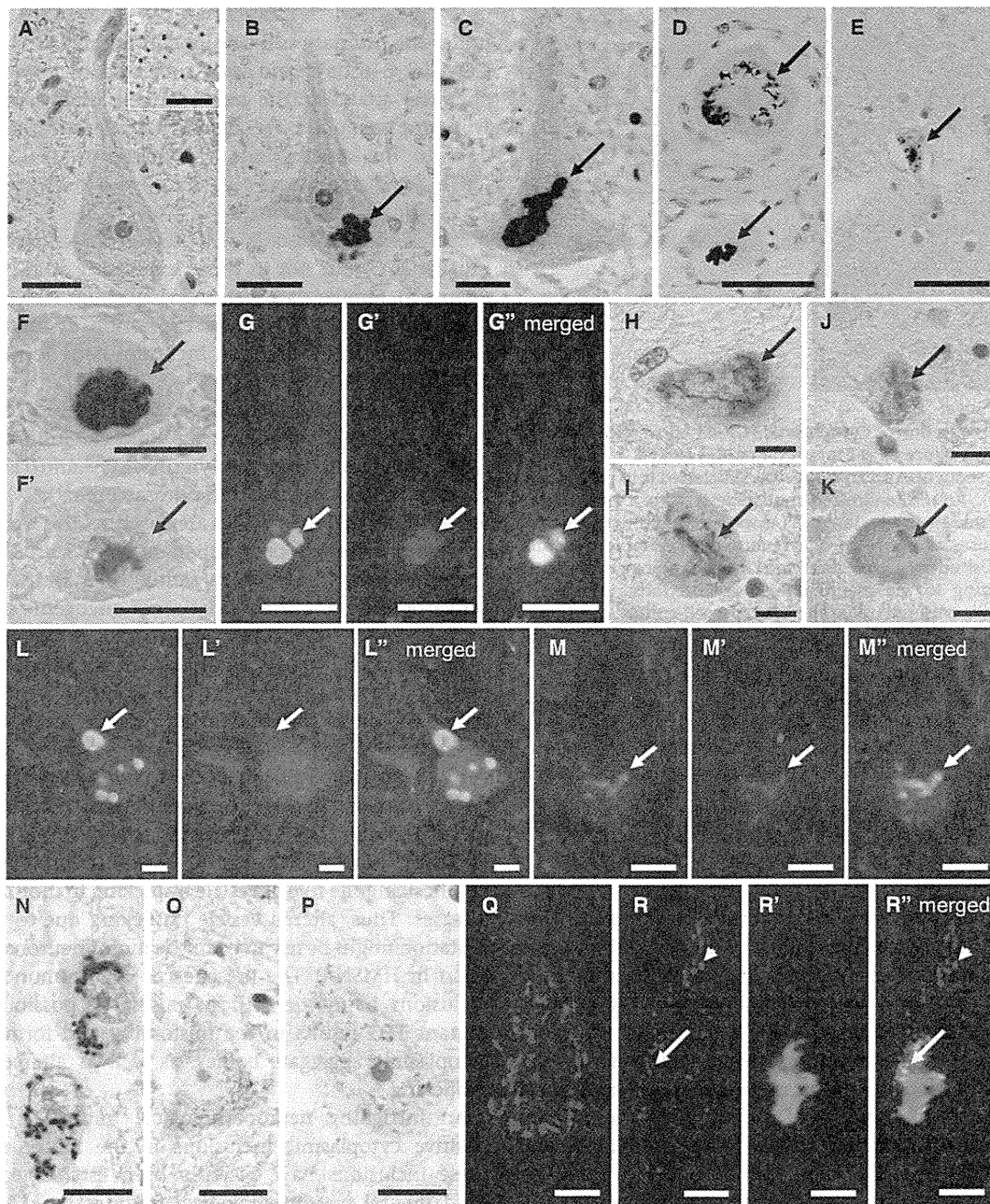
Figure 4. TFG-Related Neuropathological Findings

(A) TFG immunostaining (with hematoxylin counterstaining) of a motor neuron in the spinal cord of a neurologically normal control. A high-power magnified photomicrograph (inset) shows fine granular staining of TFG in the cytoplasm. The scale bars represent 20 μm (main panel) and 10 μm (inset).

(B–E) TFG-immunopositive inclusions of the neurons (with hematoxylin counterstaining) in the hypoglossal nucleus (B), anterior horn of the spinal cord (C), dorsal root ganglion (D, arrows), and motor cortex (E, arrow) of the patient with the *TFG* mutation. The scale bars represent 20 μm (B–D) and 50 μm (E).

(F and F') Serial section analysis of the facial nucleus motor neuron showing an inclusion body colabeled for TFG (F) and ubiquitin (F'). The scale bars represent 20 μm.

(G–G") Double immunofluorescence microscopy confirming colocalization of TFG (green) and ubiquitin (red) in an inclusion body of a motor neuron in the hypoglossal nucleus. The scale bars represent 20 μm.

(H and I) TDP-43-positive skein-like inclusions in the motor neurons of the abducens nucleus (H) and anterior horn of the lumbar cord (I). The scale bars represent 20 μm.

(J and K) Phosporylated TDP-43-positive inclusion bodies in the cervical anterior horn (J) and Clarke's nucleus (K). The scale bars represent 20 μm.

(L–L") Round inclusions (arrows) positive for TFG (green) but negative for TDP-43 (red). The scale bars represent 20 μm.
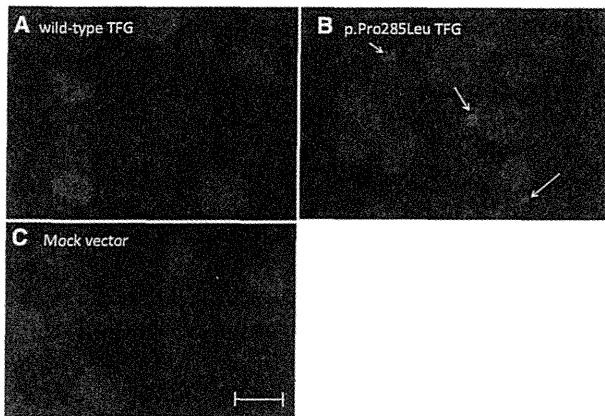
Figure 5. Formation of Cytoplasmic TDP-43 Aggregation Bodies in Cells Stably Expressing Mutant p.Pro285Leu TFG
The coding sequence of *TFG* cDNA was subcloned into pBluescript (Stratagene). After site-directed mutagenesis with a primer pair shown in Table S9, the mutant cDNAs were cloned into the BamHI and XhoI sites of pcDNA3 (Life Technologies). Stable cell lines were established by Lipofectamine (Life Technologies) transfection according to the manufacturer's instructions. Established cell lines were cultured under the ordinary cell-culture conditions (37°C and 5% CO_2) for 5–6 days and were subjected to immunocytochemical analyses. Neuro-2a cells stably expressing wild-type TFG (A), mutant TFG (p.Pro285Leu) (B), and a mock vector (C) are shown. TDP-43-immunopositive cytoplasmic inclusions are absent in the cells stably expressing wild-type TFG or the mock vector (A and C); however, TDP-43-immunopositive cytoplasmic inclusions were exclusively demonstrated in cells stably expressing mutant TFG (p.Pro285Leu), as indicated by arrows (B). Similar results were obtained with HEK 293 cells (not shown). Scale bars represent 10 μm.

a TGN46 antibody. It revealed that the Golgi apparatus was fragmented in approximately 70% of the remaining motor neurons in the lumbar anterior horn. The fragmentation of the Golgi apparatus was prominent near TFG-positive inclusion bodies (Figures 4N–4R). In summary, we found abnormal TDP-43-immunopositive inclusions in the cytoplasm of motor neurons, as well as fragmentation of the Golgi apparatus in HMSN-P, confirming the overlapping neuropathological features between HMSN-P and sporadic ALS.

To further investigate the effect of mutant TFG in cultured cells, stable cell lines expressing wild-type and mutant TFG (p.Pro285Leu) were established from neuro-2a and human embryonic kidney (HEK) 293 cells as previ-

ously described.[18] Established cell lines were cultured under the ordinary cell-culture conditions (37°C and 5% CO_2) for 5–6 days and were subjected to immunocytochemical analyses. The neuro-2a cells stably expressing wild-type or mutant TFG demonstrated no distinct difference in the distribution of endogenous TFG, FUS, or OPTN (data not shown). In contrast, cytoplasmic inclusions containing endogenous TDP-43 were exclusively observed in the neuro-2a cells stably expressing untagged mutant TFG, but not in those expressing wild-type TFG (Figure 5). Similar data were obtained from HEK 293 cells (data not shown). Thus, the expression of mutant TFG leads to mislocalization and inclusion-body formation of TDP-43 in cultured cells.

TFG was originally identified as a part of fusion oncoproteins (NTRK1-T3 in papillary thyroid carcinoma,[19] TFG-ALK in anaplastic large cell lymphoma,[20] and TFG/NOR1 in extraskeletal myxoid chondrosarcoma[21]), where the N-terminal portions of TFG are fused to the C terminus of tyrosine kinases or a superfamily of steroid-thyroid hormone-retinoid receptors acting as a transcriptional activator leading to the formation of oncogenic products. Very recently, TFG-1, a homolog of TFG in *Caenorhabditis elegans*, and TFG have been discovered to localize in endoplasmic-reticulum exit sites. TFG-1 acts in a hexameric form that binds the scaffolding protein Sec16 complex assembly and plays an important role in protein secretion with COPII-coated vesicles.[22] It is noteworthy that mutations in genes involved in vesicle trafficking[23,24] (such genes include *VAPB*, *CHMP2B*, *alsin*, *FIG4*, *VPS33B*, *PIP5K1C*, and *ERBB3*) cause motor neuron diseases, emphasizing the role of vesicle trafficking in motor neuron diseases. Thus, altered vesicle trafficking due to the *TFG* mutation might be involved in the motor neuron degeneration in HMSN-P. The presence of TFG-immunopositive inclusions in motor neurons raises the possibility that mutant TFG results in the misfolding and formation of cytoplasmic aggregate bodies, as well as altered vesicle trafficking.

An intriguing neuropathological finding is TDP-43-positive cytoplasmic inclusions in the motor neurons; these inclusions have recently been established as the fundamental neuropathological findings in ALS.[13,14] Of note, expression of mutant, but not wild-type, TFG in cultured cells led to the formation of TDP-43-containing cytoplasmic aggregation. These observations are similar

(M–M″) An inclusion immunopositive for both TFG (green) and TDP-43 (red) is observed in a small number of neurons. The scale bars represent 20 μm.
(N) Normal Golgi apparatus in the neurons of the intact thoracic intermediolateral nucleus. The scale bar represents 20 μm.
(O and P) Fragmentation of the Golgi apparatus with small, round, and disconnected profiles in the affected motor neurons of the lumbar anterior horn. The scale bars represent 20 μm.
(Q–R″) Immunohistochemical observations of the Golgi apparatus and TFG-immunopositive inclusions employing antibodies against TGN46 (red) and TFG (green), respectively. The scale bars represent 10 μm.
(Q) Normal size and distribution (red) in a motor neuron without inclusions.
(R–R″) The Golgi apparatus was fragmented into various sizes and reduced in number in the lumbar anterior horn motor neuron with TFG-positive inclusions (green). The fragmentation predominates near the inclusion (arrow), whereas the Golgi apparatuses distant from the inclusion showed nearly normal patterns (arrow head).

–31–

to what has been described for ALS, where TDP-43 is mislocalized from the normally localized nucleus to the cytoplasm with concomitant cytoplasmic inclusions. Cytoplasmic TDP-43 accumulation and inclusion formation have also been observed in motor neurons in familial ALS with mutations in *VAPB* (MIM 608627) or *CHMP2B* (MIM 600795).[25,26] Furthermore, TDP-43 pathology has been demonstrated in transgenic mice expressing mutant VAPB.[27] Although the mechanisms of mislocalization of TDP-43 remain to be elucidated, these observations suggest connections between alteration of vesicle trafficking and mislocalization of TDP-43. Thus, common pathophysiologic mechanisms might underlie motor neuron degenerations involving vesicle trafficking including TFG, as well as VAPB and CHMP2B. Because TDP-43 is an RNA-binding protein, RNA dysregulation has been suggested to play important roles in the TDP43-mediated neurodegeneration.[28] Furthermore, recent discovery of hexanucleotide repeat expansions in *C9ORF72* in familial and sporadic ALS/FTD (MIM 105550)[29,30] emphasizes the RNA-mediated toxicities as the causal mechanisms of neurodegeneration. Observations of TDP-43-positive cytoplasmic inclusions in the motor neurons of the patient with HMSN-P raise the possibility that RNA-mediated mechanisms might also be involved in motor neuron degeneration in HMSN-P.

In summary, we have found that *TFG* mutations cause HMSN-P. The presence of TFG/ubiquitin- and/or TDP-43-immunopositive cytoplasmic inclusions in motor neurons and cytosolic aggregation composed of TDP-43 in cultured cells expressing mutant TFG indicate a novel pathway of motor neuron death.

Supplemental Data

Supplemental Data include three figures and nine tables and can be found with this article online at http://www.cell.com/AJHG/.

Acknowledgments

Web Resources

The URLs for data presented herein are as follows.

1000 Genomes Project Database, http://www.1000genomes.org/
dbSNP, http://www.ncbi.nlm.nih.gov/projects/SNP/
HapMap, http://hapmap.ncbi.nlm.nih.gov/
NHLBI GO Exome Sequencing Project, https://esp.gs.washington.edu/drupal/
Online Mendelian Inheritance in Man (OMIM), http://www.omim.org
PolyPhen, http://genetics.bwh.harvard.edu/pph/
RefSeq, http://www.ncbi.nlm.nih.gov/projects/RefSeq/
UCSC Human Genome Browser, http://genome.ucsc.edu/

References

1. Takashima, H., Nakagawa, M., Nakahara, K., Suehara, M., Matsuzaki, T., Higuchi, I., Higa, H., Arimura, K., Iwamasa, T., Izumo, S., and Osame, M. (1997). A new type of hereditary motor and sensory neuropathy linked to chromosome 3. Ann. Neurol. *41*, 771–780.

2. Nakagawa, M. (2009). [Wide spectrum of hereditary motor sensory neuropathy (HMSN)]. Rinsho Shinkeigaku *49*, 950–952.

3. Maeda, K., Sugiura, M., Kato, H., Sanada, M., Kawai, H., and Yasuda, H. (2007). Hereditary motor and sensory neuropathy (proximal dominant form, HMSN-P) among Brazilians of Japanese ancestry. Clin. Neurol. Neurosurg. *109*, 830–832.

4. Patroclo, C.B., Lino, A.M., Marchiori, P.E., Brotto, M.W., and Hirata, M.T. (2009). Autosomal dominant HMSN with proximal involvement: new Brazilian cases. Arq. Neuropsiquiatr. *67* (3B), 892–896.

5. Fujita, K., Yoshida, M., Sako, W., Maeda, K., Hashizume, Y., Goto, S., Sobue, G., Izumi, Y., and Kaji, R. (2011). Brainstem and spinal cord motor neuron involvement with optineurin inclusions in proximal-dominant hereditary motor and sensory neuropathy. J. Neurol. Neurosurg. Psychiatry *82*, 1402–1403.

6. Takahashi, H., Makifuchi, T., Nakano, R., Sato, S., Inuzuka, T., Sakimura, K., Mishina, M., Honma, Y., Tsuji, S., and Ikuta, F. (1994). Familial amyotrophic lateral sclerosis with a mutation in the Cu/Zn superoxide dismutase gene. Acta Neuropathol. *88*, 185–188.

7. Maeda, K., Kaji, R., Yasuno, K., Jambaldorj, J., Nodera, H., Takashima, H., Nakagawa, M., Makino, S., and Tamiya, G. (2007). Refinement of a locus for autosomal dominant hereditary motor and sensory neuropathy with proximal dominancy (HMSN-P) and genetic heterogeneity. J. Hum. Genet. *52*, 907–914.

8. Fukuda, Y., Nakahara, Y., Date, H., Takahashi, Y., Goto, J., Miyashita, A., Kuwano, R., Adachi, H., Nakamura, E., and Tsuji, S. (2009). SNP HiTLink: A high-throughput linkage analysis system employing dense SNP data. BMC Bioinformatics *10*, 121.

9. Gudbjartsson, D.F., Thorvaldsson, T., Kong, A., Gunnarsson, G., and Ingolfsdottir, A. (2005). Allegro version 2. Nat. Genet. *37*, 1015–1016.

10. Li, H., and Durbin, R. (2009). Fast and accurate short read alignment with Burrows-Wheeler transform. Bioinformatics *25*, 1754–1760.

11. Li, H., Handsaker, B., Wysoker, A., Fennell, T., Ruan, J., Homer, N., Marth, G., Abecasis, G., and Durbin, R.; 1000 Genome Project Data Processing Subgroup. (2009). The Sequence Alignment/Map format and SAMtools. Bioinformatics *25*, 2078–2079.

12. Robinson, J.T., Thorvaldsdóttir, H., Winckler, W., Guttman, M., Lander, E.S., Getz, G., and Mesirov, J.P. (2011). Integrative genomics viewer. Nat. Biotechnol. *29*, 24–26.

13. Neumann, M., Sampathu, D.M., Kwong, L.K., Truax, A.C., Micsenyi, M.C., Chou, T.T., Bruce, J., Schuck, T., Grossman, M., Clark, C.M., et al. (2006). Ubiquitinated TDP-43 in fronto-temporal lobar degeneration and amyotrophic lateral sclerosis. Science *314*, 130–133.

14. Arai, T., Hasegawa, M., Akiyama, H., Ikeda, K., Nonaka, T., Mori, H., Mann, D., Tsuchiya, K., Yoshida, M., Hashizume, Y., and Oda, T. (2006). TDP-43 is a component of ubiquitin-positive tau-negative inclusions in frontotemporal lobar degeneration and amyotrophic lateral sclerosis. Biochem. Biophys. Res. Commun. *351*, 602–611.

15. Hasegawa, M., Arai, T., Nonaka, T., Kametani, F., Yoshida, M., Hashizume, Y., Beach, T.G., Buratti, E., Baralle, F., Morita, M., et al. (2008). Phosphorylated TDP-43 in frontotemporal lobar degeneration and amyotrophic lateral sclerosis. Ann. Neurol. *64*, 60–70.

16. Inukai, Y., Nonaka, T., Arai, T., Yoshida, M., Hashizume, Y., Beach, T.G., Buratti, E., Baralle, F.E., Akiyama, H., Hisanaga, S., and Hasegawa, M. (2008). Abnormal phosphorylation of Ser409/410 of TDP-43 in FTLD-U and ALS. FEBS Lett. *582*, 2899–2904.

17. Stieber, A., Chen, Y., Wei, S., Mourelatos, Z., Gonatas, J., Okamoto, K., and Gonatas, N.K. (1998). The fragmented neuronal Golgi apparatus in amyotrophic lateral sclerosis includes the trans-Golgi-network: Functional implications. Acta Neuropathol. *95*, 245–253.

18. Kuroda, Y., Sako, W., Goto, S., Sawada, T., Uchida, D., Izumi, Y., Takahashi, T., Kagawa, N., Matsumoto, M., Matsumoto, M., et al. (2012). Parkin interacts with Klokin1 for mitochondrial import and maintenance of membrane potential. Hum. Mol. Genet. *21*, 991–1003.

19. Greco, A., Mariani, C., Miranda, C., Lupas, A., Pagliardini, S., Pomati, M., and Pierotti, M.A. (1995). The DNA rearrangement that generates the TRK-T3 oncogene involves a novel gene on chromosome 3 whose product has a potential coiled-coil domain. Mol. Cell. Biol. *15*, 6118–6127.

20. Hernández, L., Pinyol, M., Hernández, S., Beà, S., Pulford, K., Rosenwald, A., Lamant, L., Falini, B., Ott, G., Mason, D.Y.,

et al. (1999). TRK-fused gene (TFG) is a new partner of ALK in anaplastic large cell lymphoma producing two structurally different TFG-ALK translocations. Blood *94*, 3265–3268.

21. Hisaoka, M., Ishida, T., Imamura, T., and Hashimoto, H. (2004). TFG is a novel fusion partner of NOR1 in extraskeletal myxoid chondrosarcoma. Genes Chromosomes Cancer *40*, 325–328.

22. Witte, K., Schuh, A.L., Hegermann, J., Sarkeshik, A., Mayers, J.R., Schwarze, K., Yates, J.R., 3rd, Eimer, S., and Audhya, A. (2011). TFG-1 function in protein secretion and oncogenesis. Nat. Cell Biol. *13*, 550–558.

23. Dion, P.A., Daoud, H., and Rouleau, G.A. (2009). Genetics of motor neuron disorders: New insights into pathogenic mechanisms. Nat. Rev. Genet. *10*, 769–782.

24. Andersen, P.M., and Al-Chalabi, A. (2011). Clinical genetics of amyotrophic lateral sclerosis: What do we really know? Nat Rev Neurol *7*, 603–615.

25. Ince, P.G., Highley, J.R., Kirby, J., Wharton, S.B., Takahashi, H., Strong, M.J., and Shaw, P.J. (2011). Molecular pathology and genetic advances in amyotrophic lateral sclerosis: an emerging molecular pathway and the significance of glial pathology. Acta Neuropathol. *122*, 657–671.

26. Cox, L.E., Ferraiuolo, L., Goodall, E.F., Heath, P.R., Higginbottom, A., Mortiboys, H., Hollinger, H.C., Hartley, J.A., Brockington, A., Burness, C.E., et al. (2010). Mutations in CHMP2B in lower motor neuron predominant amyotrophic lateral sclerosis (ALS). PLoS ONE *5*, e9872.

27. Tudor, E.L., Galtrey, C.M., Perkinton, M.S., Lau, K.-F., De Vos, K.J., Mitchell, J.C., Ackerley, S., Hortobágyi, T., Vámos, E., Leigh, P.N., et al. (2010). Amyotrophic lateral sclerosis mutant vesicle-associated membrane protein-associated protein-B transgenic mice develop TAR-DNA-binding protein-43 pathology. Neuroscience *167*, 774–785.

28. Lee, E.B., Lee, V.M., and Trojanowski, J.Q. (2012). Gains or losses: Molecular mechanisms of TDP43-mediated neurodegeneration. Nat. Rev. Neurosci. *13*, 38–50.

29. DeJesus-Hernandez, M., Mackenzie, I.R., Boeve, B.F., Boxer, A.L., Baker, M., Rutherford, N.J., Nicholson, A.M., Finch, N.A., Flynn, H., Adamson, J., et al. (2011). Expanded GGGGCC hexanucleotide repeat in noncoding region of C9ORF72 causes chromosome 9p-linked FTD and ALS. Neuron *72*, 245–256.

30. Renton, A.E., Majounie, E., Waite, A., Simón-Sánchez, J., Rollinson, S., Gibbs, J.R., Schymick, J.C., Laaksovirta, H., van Swieten, J.C., Myllykangas, L., et al; ITALSGEN Consortium. (2011). A hexanucleotide repeat expansion in C9ORF72 is the cause of chromosome 9p21-linked ALS-FTD. Neuron *72*, 257–268.

第3章 各 論

Charcot-Marie-Tooth 病 1. 病態・治療

要旨

Charcot-Marie-Tooth 病（CMT）は，最も頻度の高い遺伝性ニューロパチーであり，40 個以上の原因遺伝子が特定されている．CMT の中で最も多い CMT1A に関して，*PMP22* の発現抑制化合物の研究や "network pharmacology" による治療薬の開発が注目されている．我が国を中心に，ロボットスーツ HAL® の医師主導臨床治験が計画されている．外科的治療，リハビリテーション，装具療法，日常生活上の工夫も機能維持・改善にとって重要である．

● キーワード

CMT の病態に
基づいた治療戦略
内科的治療法
外科的治療法
リハビリテーション
日常生活上の注意

Charcot-Marie-Tooth 病（CMT）の臨床症状とその病態

Charcot-Marie-Tooth 病（CMT）は，1886 年に J M. Charcot，P. Marie，H H. Tooth によって報告された最も頻度の高い遺伝性ニューロパチーである．CMT はすべての人種に認められ，その有病率は，欧米ではこれまで 2,500 人に 1 人と言われてきた．最近の疫学調査でも，人口 10 万人 対 9.7 ～ 82.4 人とその頻度は高い[1]．我が国では人口 10 万人 対 10.8 人との報告があるが[2]，実際の有病率はより高いものと推定される．

CMT の多くは 0 ～ 20 歳頃までに発症するが，50 歳代の発症も比較的多い（図 1）．厚労省難治性疾患克服研究事業報告によれば，車いす使用患者は約 20 %，寝たきり患者は 1 % とされている[3]．CMT は正中神経の運動神経伝導速度（MNCV）38 m／秒を基準に，脱髄型（CMT1／CMT4），軸索型（CMT2），中間型（Intermediate-CMT）に大別される．CMT の原因遺伝子は 40 種類以上が特定され（http://www.molgen.ua.ac.be/CMTMutations）[4]，我が国においても，CMT の遺伝子診断に関しては大きな進展が見られている[5]．Choi らはエキソーム解析法により，通常の DNA 解析法では異常を見いだせなかっ

図1　Charcot-Marie-Tooth 病（CMT）自験例 55 例の発症年齢の分布
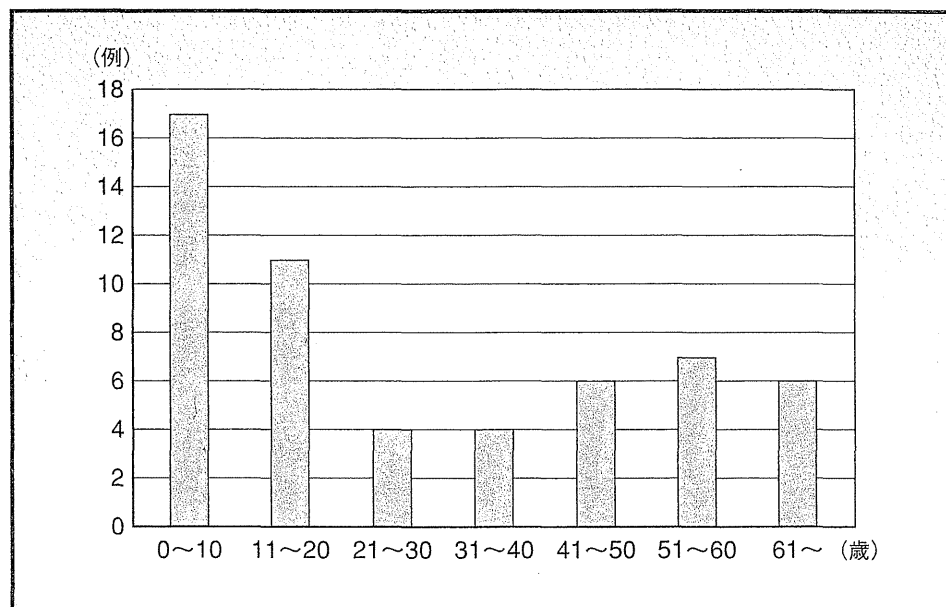
た 25 例中 8 例（32 %）に，遺伝子異常を検出したと報告している[6]．今後は，次世代シークエンサーを用いたエキソーム解析が主流になると考えられる．

　CMT の基本的病態は，原因遺伝子の変異により正常な末梢神経機能の維持が障害されることである．CMT の分子異常は，遺伝子の転写制御，タンパク代謝，シュワン細胞・軸索相互作用，軸索輸送，ミトコンドリアの分裂・融合などに異常を引き起す（図2）[4][7]．また，*PMP22, MPZ, periaxin* などの CMT 原因遺伝子は，末梢神経に特異的発現しており，末梢神経特異的機能障害に関与している．一方，*GARS, HSP27, GJB1*（*Cx32*）などは多数の臓器で発現しているが，末梢神経組織で特異的な役割を担っていることが明らかとなった．

　末梢神経の中でも，*GARS, YARS* などはタンパク合成阻害作用，*HSP22, HSP27* などはストレス反応異常，アポトーシス異常，軸索輸送障害を通じて，運動神経優位な障害を惹起する．*SPTLC1, DNMT1, RAB7* などは細胞内タンパク輸送・タンパク代謝障害などにより，感覚神経優位の障害を引き起す．シュワン細胞・ミエリンと神経細胞・軸索間の分子相互関係の解明が，分子病態に基づいた治療法の開発へつながっていくと考えられる．最近，"network pharmacology（ネットワーク薬理学）" というバイオインフォマティクスに基づく新しい治療薬開発法が注目されている．後述するように，このネットワ

図2　Charcot-Marie-Tooth 病（CMT）関連遺伝子とその発現部位
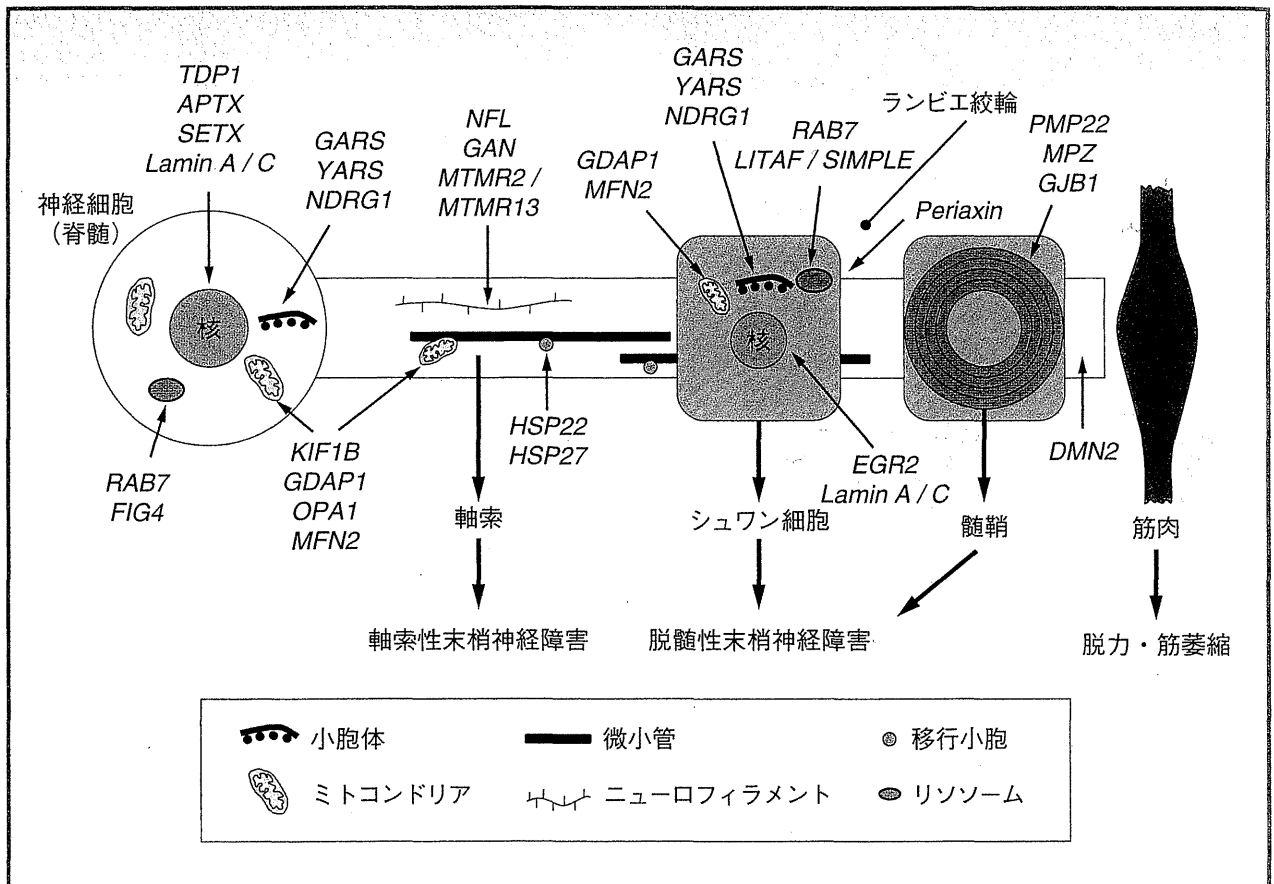
ーク薬理学からデザインされた CMT1A の治療法開発が進められている．CMT の分子病態解明は，末梢神経障害にとどまらず，広く神経変性疾患全体の病態解明につながっていくと考えられる．

Charcot-Marie-Tooth 病（CMT）に対する薬物治療

1．CMT1A の薬物療法

PMP22 の重複によって引き起される CMT1A は最も頻度が高く，種々の治療法が試みられている．

1）アスコルビン酸臨床試験

アスコルビン酸は，後根神経節-シュワン細胞の培養系におけるmyelination に必須であり，アスコルビン酸欠乏が大腿神経障害を引き起すことが報告されている[8]．アスコルビン酸は cAMP の CREBへの結合を競合的に阻害し，PMP22 mRNA 発現量を低下させる可能性がある．アスコルビン酸が CMT1A モデルマウスに有効であるとの報告があり[9]，国内外で臨床試験が行われた．

我が国でも「Charcot-Marie-Tooth 病 1A に対するアスコルビン酸の安全性・有効性に関する臨床試験」（UMIN 試験 ID：UMIN000001535）が投与群と非投与群によるオープン試験として行われた[10]．プライマリーエンドポイントである CMT ニューロパチースコア（CMTNS）に有意な改善はなく，アスコルビン酸の有効性は確認できなかった．海外でのアスコルビン酸投与試験でも，我が国の研究班の結果と同様に，アスコルビン酸の有効性は証明されなかった[11]．しかし，Burns らは，アスコルビン酸臨床試験後に 12 ヵ月の追加オープン試験を 20 歳未満の 5 例に行い，複合運動活動電位（CMAP）は減少したが，四肢遠位部の筋力は有意に改善したと報告している．比較的軽症の若年 CMT1A 患者には，アスコルビン酸の長期大量投与が有効である可能性が示唆された[12]．我が国のアスコルビン酸臨床試験でも，右握力は有意に改善していた．現在，Qtrac プログラム（ミユキ技研）を用いて，アスコルビン酸投与前後での軸索興奮性を検討中である．

ニュートロピン-3（NT-3），プロゲステロン拮抗薬などが CMT1A の治療に有効である可能性が報告されているが，十分なエビデンスはない．最近，培養細胞に *PMP22* を発現させ，その発現を抑制する化合物をオートマチックにスクリーニングするハイスループットな方法が開発されている[10]．

2）クルクミンによる CMT 治療

クルクミンは秋ウコンやカレー粉に多く含まれている自然の黄色色素である．クルクミンは変異 PMP22 タンパクを細胞膜へ解放し，変異 *PMP22* 発現によるアポトーシスを減少させることが報告されている．動物レベルにおいても，クルクミンは用量依存的に運動機能を改善し，坐骨神経の軸索径を増加させ，シュワン細胞のアポトーシスを減少させている．以上の検討から，クルクミンが *pmp22* 点変異マウスに有効であることが示された[13]．Burns らは，*PMP22* 点変異（Ser72Leu）を有する 15 歳女性例にクルクミンカプセルを 12 ヵ月間経口投与し，評価指標の改善はなかったが，幸福感，満足感に関する自覚的な改善があったと報告している[14]．

2．バイオマーカーの開発

患者数が少ない CMT の場合，臨床試験デザインについても検討

する必要がある．最近の無作為化臨床試験では，皮膚生検による末梢神経の形態および mRNA 発現の評価が行われているが，今後，新しいサロゲートマーカーの開発も必要である．Fledrich らは，CMT1A ラットモデルの坐骨神経と皮膚組織の mRNA 解析や 46 例の CMT1A 患者の皮膚生検の mRNA 解析から，*glutathione S-transferase theta 2* と *cathepsin A* の mRNA レベルが CMT1A の軸索障害のバイオマーカーになる可能性を示した[15]．

3．Network pharmacology

"Network pharmacology" という bioinformatics に基づく新しい治療薬開発法が注目されている．Pharnext 社が CMT1A60 例を対象に PXT3003（バクロフェン，naltrexone，ソルビトールの合剤）の治験を 2010 年から行っている．2012 年末には治験結果が発表される予定である[16]．この治験の結果によっては，ほかの CMT に対しても network pharmacology に基づく新たな創薬が期待される．

4．モデル動物を用いた治療法の開発

CMT のモデル動物による研究も進展しており，脱髄型 CMT では，約 25 種類の動物モデルが報告されている（http://www.molgen.ua.ac.be/CMT Mutations)[17]．TrkB / TrkC に対する作動性抗体，間葉系幹細胞，ドキシサイクリン，Colony-stimulating factor-1，histone deacetylase 6 阻害薬，バルプロ酸，*MFN1* 発現増加作用などが，特定の遺伝子変異による CMT 治療に有効である可能性が報告されている．CMT のモデル動物による治療法の開発研究は大きく進歩しており，その研究成果が臨床に応用される日が待たれる．

5．投与に注意したほうがよい薬物

使用される薬剤が CMT の症状を悪化させる場合がある（http://www.charcot-marie-tooth.org/med_alert.php)．最近，抗がん化学治療薬の投与により末梢神経障害が顕在化し，CMT の遺伝子変異が明らかとなった例が報告されている[18]．CMT の臨床症状を示さない潜在的な CMT 患者がいる可能性があり，抗腫瘍薬（ビンクリスチンなど）投与前の神経伝導検査の実施は，末梢神経障害の重症化を防ぐ点で可能な限り推奨される．

炎症性ニューロパチーと Charcot-Marie-Tooth 病（CMT）

CMT1A を代表とする遺伝性ニューロパチーと慢性炎症性脱髄性多発神経炎（CIDP）との合併例の検討から，CMT 患者 250 人に 1 人が CIDP 様の炎症性ニューロパチーを発症すると推定されている．CMT 患者で臨床症状の急性悪化を認めた場合には，CIDP などの炎症性ニューロパチーの治療法に準じた対応を考慮すべきである[19]．

外科治療

症状の進行に伴い，筋延長術や骨切り術などの整形外科手術が適応となる場合がある．Leeuwesteijn らは，CMT 33 例（男性 14 例，女性 19 例）の術後平均 56.9 ヵ月の評価を行い，疼痛，歩行障害が有意に改善し，90 % の患者が足変形の矯正に満足していたと報告している[20]．内反尖足の外科治療は，CMT 患者により安定した歩行をもたらすと考えられるが，その手術適応や外科的治療施行時期についての基準作成が必要とされている[21]．

リハビリテーション

「運動し過ぎは良くないでしょうか？」と CMT 患者または家族から尋ねられることが多い．"過労による筋力低下（overwork weakness）" についてはこれまでも論議が多い．CMT の症状が軽症である例では，利き手の握力とピンチ力が非利き手より強い傾向があるが，重症例では，利き手のピンチ力が非利き手よりも有意に低下していると報告されている[22]．CMT の関節可動域制限の予防のために，発症早期から下腿三頭筋の持続伸張訓練を行うことが勧められている．Maggi らは，CMT 8 例にトレッドミル，ストレッチ，呼吸，固有受容器刺激訓練を週 2 回，8 週間行ったところ，足関節角度および 6 m 歩行時間の改善を認めたと報告している[23]．日々の生活に運動療法を組み込むことで，疾患の自然経過による進行以上の悪化を抑える効果が期待できる．

装具療法

病状に適合した装具使用は有効である．Guillebastre らは，CMT 26例を対象に，普通靴，プラスティック短下肢装具，エラスティックバン短下肢装具の効果を比較した．その結果，短下肢装具の使用は歩行と姿勢の異常を部分的に改善したと報告している[24]．

Charcot-Marie-Tooth 病 (CMT) に対する ロボット技術の応用

レジーナ®（日本ロジックマシン），ロボットスーツ HAL®（筑波大学，Hybrid Assistive Limb：HAL）などのロボット技術の活用も期待される．HAL®は，近位筋の障害もある重度障害の CMT 患者に適応があることが報告された[25]．2011 年度に厚生労働省難治性疾患克服研究事業として，「希少性難治性疾患—神経・筋難病疾患の進行抑制治療効果を得るための新たな医療機器，生体電位などで随意コントロールされた下肢装着型補助ロボット（HAL-HN01）に関する 医師主導治験の実施研究」班（研究代表者 中島 孝先生）が組織され，補助ロボット技術の本格的な臨床治験が始まろうとしている．

Charcot-Marie-Tooth 病 (CMT) 患者の日常生活の工夫

CMT に対する有効な薬物療法はいまだ開発されていないが，少しでも良い健康状態を維持するために，日常的な運動習慣と食事療法が大切である．CMT 患者は消費カロリー／日が健常者より有意に少なく，メタボリックシンドロームが多い傾向が見られる．"現在の体重を維持する" こと，四肢遠位の冷感・浮腫，外傷，胼胝や潰瘍の形成に注意すること，深部静脈血栓症とそれに関連する肺塞栓症に注意することなどが必要である[26]．

おわりに

欧米に比べると我が国では，CMT に対する医療従事者および一般社会の認知が不十分であり，単純に「CMT の治療法はない」と考えている医療関係者，CMT 患者が多いのではないかと思われる．最近，厚生労働省研究班により『シャルコー・マリー・トゥース病診療マニ